Influence of the footprint of resonant additions on the stop band behaviour of 1D locally resonant metamaterials.

Alves Pires, Felipe[1]
KU Leuven, Dept. of Mechanical Engineering and DMMS Lab, Flanders Make
Celestijnenlaan 300, B-3001, Leuven, Belgium

Claeys, Claus[2]
KU Leuven, Dept. of Mechanical Engineering and DMMS Lab, Flanders Make
Celestijnenlaan 300, B-3001, Leuven, Belgium

Deckers, Elke[3]
KU Leuven, Dept. of Mechanical Engineering and DMMS Lab, Flanders Make
Celestijnenlaan 300, B-3001, Leuven, Belgium

Desmet, Wim[4]
KU Leuven, Dept. of Mechanical Engineering and DMMS Lab, Flanders Make
Celestijnenlaan 300, B-3001, Leuven, Belgium

ABSTRACT

Due to trends towards the use of lightweight structures, novel low mass and compact NVH solutions are necessary in order to tackle the challenges of not only achieving a good NVH reduction performance but also the lightweight imposed requirements. Metamaterials have been ensuring proven to hold great potential to enhance the vibro-acoustic response of several engineering applications. They are made from conventional materials and due to the dynamic interaction between resonant additions and the host structure, metamaterials can create stop band behaviour, i.e. frequency zones of strong vibration and/or noise attenuation. Various design parameters have been shown to have influence on the achieved stop bands. One of these design parameters is the footprint of the resonant addition e.g. the size of the contact area between the resonant addition and the host structure. The present paper investigates numerically and experimentally the influence of the footprint on the stop bands by using 1D finite metamaterial structures. It is shown that this design parameter affects both the stop bands width as well as the stop band location in the frequency domain.

Keywords: metamaterials, stop bands, footprint
I-INCE Classification of Subject Number: 41, 42, 46

---

[1] felipe.alvespires@kuleuven.be

[2] claus.claeys@kuleuven.be

[3] elke.deckers@kuleuven.be

[4] wim.desmet@kuleuven.be

1. INTRODUCTION

The development of novel Noise, Vibration and Harshness (NVH) solutions for engineering applications is of key importance and due to trends towards the use of lightweight structures, novel low mass and compact NVH solutions are required in order to tackle the challenges of not only achieving a good NVH reduction performance but also ensuring lightweight design. Metamaterials have been investigated and proven to hold great potential to enhance the vibro-acoustic response of several engineering applications [1, 2, 3, 4].

Metamaterials are defined as materials that are engineered from conventional materials in order to have properties that cannot be found in nature. These unconventional properties do not come directly from the composition itself but come from the interaction between the elements on the scale of the resulting material [5]. These metamaterials have the potential to create stop bands, or band gaps, which are frequency zones where there is no free propagation of waves.

There are two different stop band formation mechanisms: interference based and resonance based. The latter can be achieved by adding resonant inclusions, also known as resonators, to a host structure on a subwavelength scale [6], keeping in mind that these resonant inclusions can only create stop bands as long as the net sum of the forces contributed by a resonator to the hosting system is non-zero [7]. These zones of pronounced attenuation result from a Fano-type interference and they can be predicted by making use of dispersion diagrams, which can be calculated by a unit cell (UC) modelling utilizing a finite element (FE) model together with the application of Bloch's theorem and evaluating the so-called Brillouin zones [8, 9, 10, 11].

Various aspects and parameters have been shown to have an effect on these stop bands such as damping properties of the constituent materials and the shape of these metamaterial inclusions [12, 13]. Additionally, the influence of boundary conditions and the way they affect stop bands have also been investigated [14]. This paper has the aim to investigate another parameter that has an influence on resonance based stop bands. The feature considered here is the contact area between the inclusions on the host structure, in order words, the footprint that the resonators have on the host structure. This feature is studied by investigating 1D metamaterial beams. At first, some theoretical insights are given by using TVAs (tuned vibration absorbers) and later experimental results are shown in order to validate the findings of the theoretical approach for a real life realization.

2. EXPLOITING THE FOOTPRINT

In order to help understand the concept of exploiting the footprint of resonators and its influence on stop bands, an academic approach is used by utilizing TVAs (tuned vibration absorbers). These systems can be understood as single degree of freedom mass-spring systems (SDOF). Due to the existence of a localized resonance, they can lead to a stop band when added periodically on a subwavelength scale onto a host structure. By using periodicity, the designs can be based on UC models, which represent infinite structures [6, 9].

Figure 1 illustrates examples of TVAs with different footprints. By tuning the springs, these resonators can be tailored to the same resonance frequency, but one can see that they occupy a different area inside the UC. The single TVA on the left occupies only one single point on the UC whereas the modified TVA with more added springs on the right occupies a bigger and square area. It is worth mentioning that, in the analysis, the amount of added mass by the resonant addition is kept the

same and for the modified TVA, the total stiffness of all springs are kept the same such that always the same tuned resonance frequency is achieved, since the springs are considered to be in parallel to each other. The stiffness k of each spring is then $k_{new} = k_{original}/n$, where n is the number of added springs and $k_{original}$ is the stiffness of the original spring.
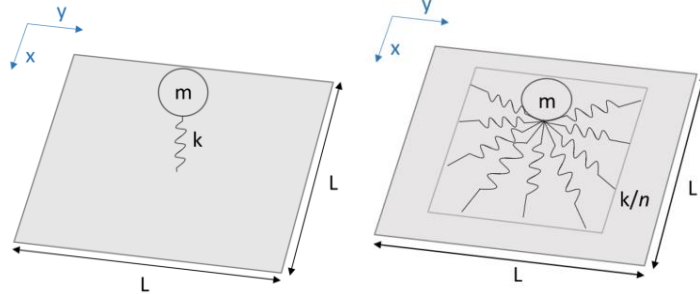
Figure 1: SDOF mass-spring system on a UC of length L (Left) single TVA (Right) modified TVA occupying a square area.

As a way of quantifying this footprint, percentage ratios are used according to the area the addition occupies in the UC. For instance, a 1-spring TVA as in Figure 1 is evaluated as having 0% of footprint, as they are fixed only in one point. Similarly, a modified resonator that occupies a square area of 64% w.r.t. the entire area of the UC is evaluated as having 64% of footprint, e.g. if $A_{UC} = 50x50$ mm^2, the area that the resonator occupies is $A_{res} = 40x40$ mm^2. Hence, as the value of footprint increases, the number of springs also increases.

As an example, Figure 2 illustrates the stop bands created by using both single and modified TVAs with 0% and 64% of footprint, respectively, tuned to the same resonance frequency and with same mass addition. The points O-A-B-O represent the Irreducible Brillouin Contour (IBC) [15]. The test case considers a host structure made of steel with a unit cell of length L = 50 mm and thickness t = 5 mm. The material properties are shown in Table 1. The resonant addition is tuned to 2000 Hz in order to be in a sub-wavelength scale, with a frequency ratio $f_{res}/f_{\lambda/2} = 0.4$ [1, 5], considering 20% of mass addition by the TVA w.r.t the UC mass.

For the case of 0% footprint TVA, no free wave propagation is found around the frequency to which the TVA is tuned, indicating a resonance based stop band. It ranges from 1956 – 2172 Hz, being 216 Hz wide. On the other hand, for the case of 64% footprint TVA, even though the TVA is tuned to the same frequency as before, the stop band region is slightly shifted to higher frequencies, in this case ranging from 1991 - 2191 Hz, being 200 Hz wide and, consequently, 16 Hz narrower as compared to the first case. This happens due to the distribution of reaction forces by the TVA throughout the UC.

This approach provides an analysis closer to real-life applications since in reality there would not be a resonant addition occupying only a single point on the host structure but resonators that occupy a certain area in the system.

Table 1: Material properties of steel.

Young's Modulus	Density	Poisson's Ratio
210 GPa	7800 kg/m^3	0.3
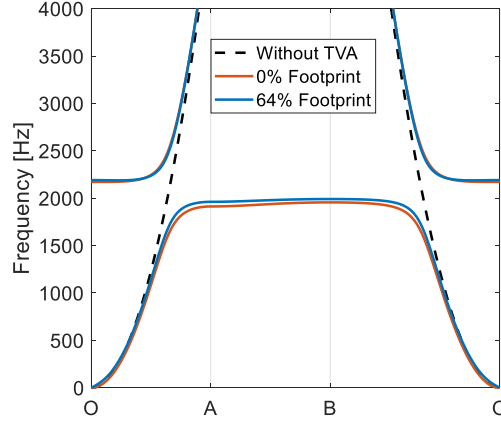
Figure 2: Comparison between dispersion diagrams between 0% and 64% of footprint resonators.

Next, an analysis is performed by changing both the footprint and the UC length L. The same conditions are applied, by tuning the resonators to 2000 Hz and keeping 20% of mass addition. Figure 3 shows the comparison of stop bands versus footprint ratio for different UC lengths.
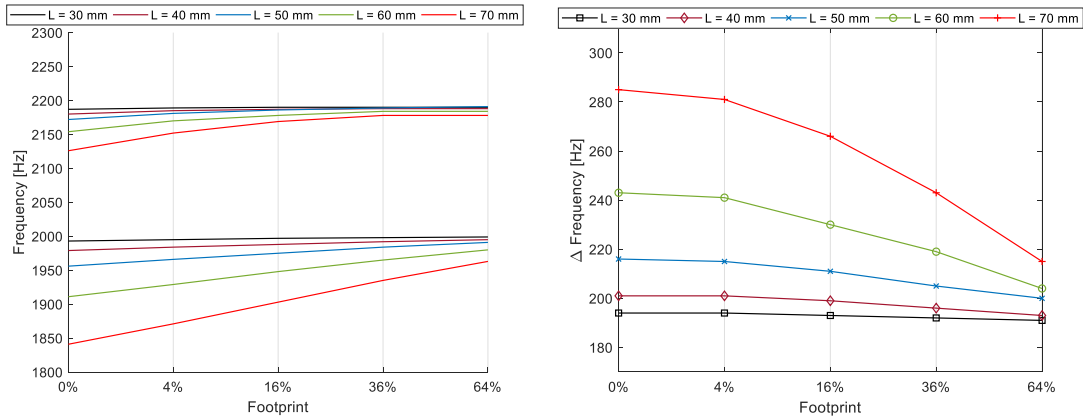
Figure 3: Comparison of stop bands as a function of the footprint for different UC lengths (Left) Stop band limits (Right) Stop band widths.

By analysing these 2 graphs together, it can be seen that there is a trend towards wider stop bands as L increases and this is due to the fact that the value of $f_{\lambda/2}$ reduces as the unit cell length grows, which results in a combination of interference based and resonance based stop bands [9]. Another common trend is the fact that the stop bands' widths decrease as the footprint values increase, as introduced earlier in this paper. This trend can be seen clearly for the case L = 70 mm, whose frequency ratio is high. Therefore, in can be concluded that the footprint that the resonant additions have inside the UC have some influence on the stop bands and this feature needs to be taken into account when designing realizable resonators. In order to have wider stop bands, the resonant additions' footprint needs to be as small as possible.

3. REALIZABLE VIBRO-ACOUSTIC METAMATERIALS WITH DIFFERENT FOOTPRINTS

As seen in the previous section, the resonant addition's footprint is influencing the predicted stop bands, not only their location in the frequency domain but also

their widths. This section has the goal of verifying experimentally the influence of the footprint on the predicted stop bands and on the response of a finite structure with attached real-life resonant additions.

3.1 Host structure

The experiments are performed in beams made of aluminium. In total, 3 beams are used: 1 as a bare case and 2 others with resonators of different footprints. These beams have dimensions 1064 x 30 x 2 mm and they are cut from the same source panel such that the material properties are the same in all cases. Unit cells of dimensions 40 x 30 x 2 mm are used in this particular case. Figure 4 illustrates the beam dimensions used in the model and in the experiments. One end of the beam is clamped and the other end is free. The free part of the beam has a length of 800 mm.
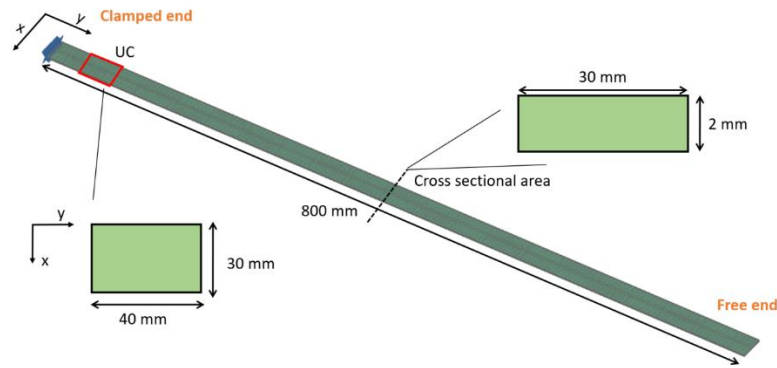
Figure 4: Beam properties used in the model and in the experiments.

A modal analysis is performed on a clamped bare beam to retrieve the material properties of the aluminium through model updating. Results are shown in Table 2.

Table 2: Material properties of the aluminium beam.

Young's Modulus	Density	Poisson's Ratio	% Structural Damping
63.14 GPa	2640.80 kg/m^3	0.34	0.01%

3.2 Designed resonators

For this study, the resonators are designed having the same features e.g. resonance frequency, added mass and modal effective mass. In addition, they are designed in a way so that their footprints can be easily changed. The parameter that changes is the length of their base, thus, their footprints can be either increased or decreased. This design approach is chosen because of its ease of analysis and manufacturability.

The proposed resonators are designed keeping also in mind that as the footprint increases, the distribution of forces by the resonators on the unit cell also increases. They are designed to be subwavelength in a frequency ratio around 0.6. The targeted frequency is 1655 Hz.

Figure 5 illustrates the designs of the resonators. Resonator type 1 has a smaller base so that it has a smaller footprint compared to resonator type 2. All resonators are made of plexiglass and are 6 mm thick (out of plane direction in Figure 5). The material properties of the plexiglass used, which have been identified in other studies [1, 3], are given in Table 3.
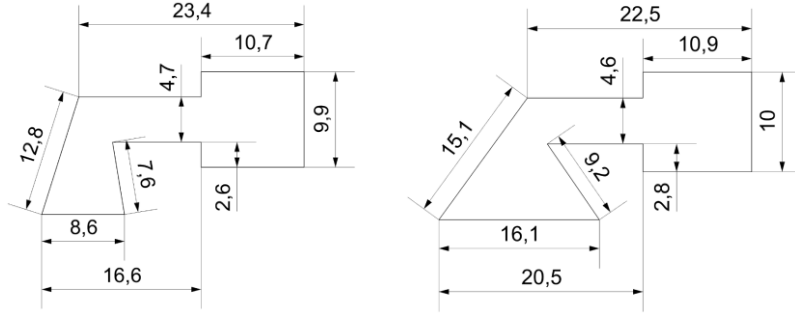
Figure 5: Resonators (Left) Type 1 (Right) Type 2.

Table 3: Material properties of the resonators.

Young's Modulus	Density	Poisson's Ratio	% Structural Damping
4850 MPa	1188.38 kg/m^3	0.31	5%

Table 4 illustrates the details of each resonator. It shows that the resonators are designed to have similar characteristics such as tuned frequency, percentage added mass and modal effective mass [16] as the footprint changes.

Table 4: Resonators features numerically acquired.

Features	Resonator 1	Resonator 2
Resonance Frequency [Hz]	1654.87	1654.77
Static mass [g]	1.57	1.79
Added mass	25%	28%
Effective mass [g]	0.81	0.83
SB limits [Hz]	1401 - 1682	1421 – 1697
SB Widths [Hz]	281	276
Footprint	21.50%	40.25%

The distribution of reaction forces in the interface between both is depicted in Figure 6. This analysis results from the analysis of the first flexural eigenmode with the resonators fully clamped on their base.
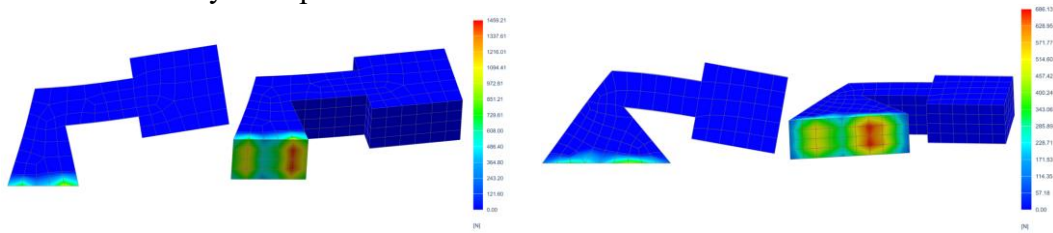
Figure 6: Distribution of forces by the resonators (Left) Type 1 (Right) Type 2.

The predicted stop bands for the respective designs of the infinite structures for 1D waveguide systems [17, 18, 19, 20] are shown in Figure 7. The stop band for type 2 is smaller and shifted to higher frequencies.
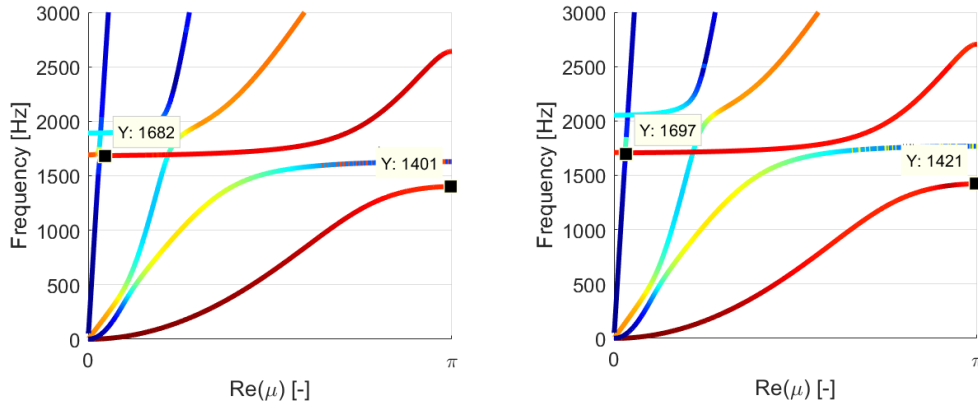
Figure 7: Predicted stop bands for the resonators (Left) Type 1 (Right) Type 2.

3.3 Realizable resonators

The resonators are laser cut (Figure 8). In order to check whether the resonance frequency of the resonators match to the ones numerically predicted, samples of each type are tested by gluing them to a metal block, rigidly connected to the stinger of a shaker, as shown in Figure 9. The velocity at the tip of the resonator's mass is measured using a polytech laser vibrometer. For each type, a mean value and the standard deviation is calculated. Table 5 shows the comparison between the simulated and measured resonance frequencies for the 2 different designs.

In Table 5, it can be seen that the measured and averaged resonance frequencies are relatively close to the design frequency and a same standard deviation is obtained for both types of resonators.
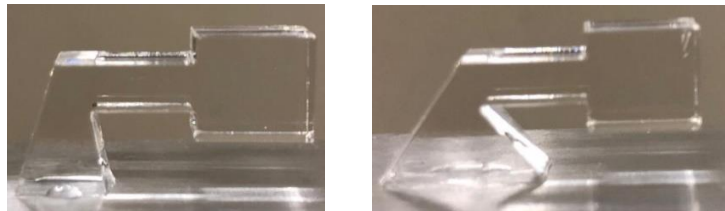
Figure 8: Samples of laser cut resonators (Left) Type 1 (Right) Type 2.

Figure 9: Test set up to retrieve the resonance frequency of the resonators.

Table 5: Comparison between the simulated and measured resonance frequencies for the 2 types of resonators.

Resonator	Numerical (Hz)	Experimental (Hz)	% Standard Deviation
Type 1	1654.87	1655.20 ± 3.66	0.22
Type 2	1654.77	1654.30 ± 3.64	0.22

3.4 Experimental set-up and results

The finite beam consists of 20 unit cells. As stated before, the free length of the beam considered in this paper is 800 mm and the UC length is 40 mm, so that a total of 20 resonators are added to each beam. On the border of each unit cell, three pieces of reflective tape are added, as illustrated in Figure 10, to acquire the vibrational response through laser vibro-measurements upon hammer excitation.
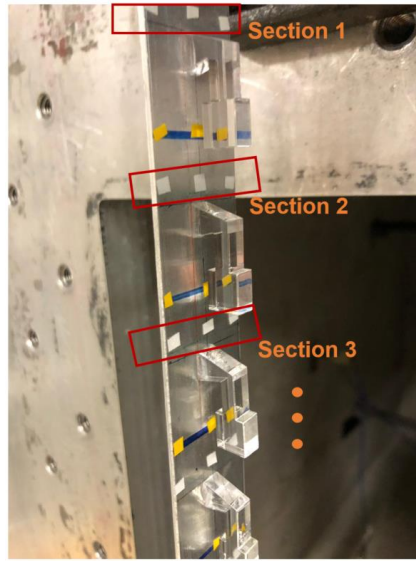
Figure 10: Sections in a metamaterial beam.

All of the resonators are placed with the centre of their base in the centre of the UC to avoid edge modes [21], as shown in Figure 11. The beams are clamped and vertically suspended, as shown in Figure 12.
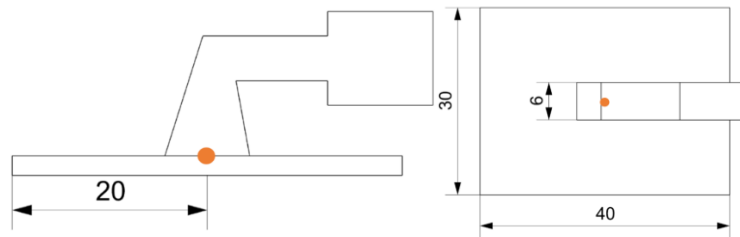
Figure 11: Example of a resonator type 1 placed on the centre of the UC.
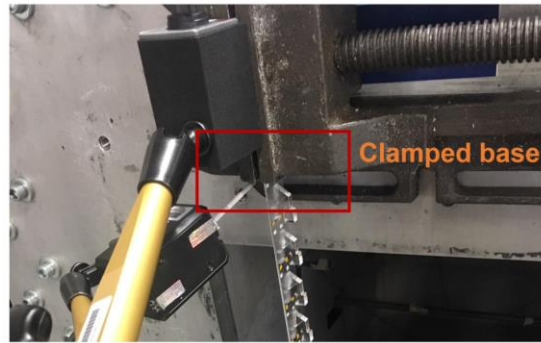
Figure 12: Beam clamped by a clamp.

The beams are excited by utilizing an automatic impact hammer, kept always in the same position so all beams are excited at the same location, as illustrated in Figure 13. An excitation point in the centre of the beam is chosen such that the flexural modes are excited while avoiding exciting the torsional modes.
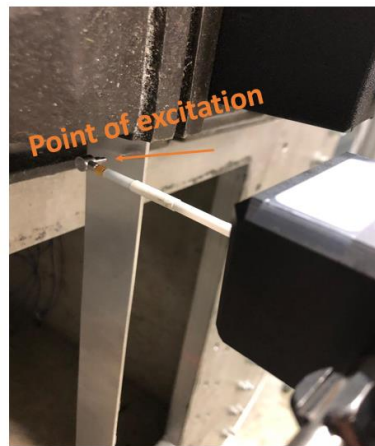
Figure 13: Automatic impact hammer set up to excite the beams.

The responses are acquired by using the PSV 500 laser vibrometer, as depicted in Figure 14, and the RMS values of all Frequency Response Function (FRF) velocity/force of each measurement point are calculated per frequency.

Figure 14: (Left) Laser vibrometer (Right) Laser beam at a point to acquire the response in a metamaterial beam.

Figure 15 depicts the comparison of FRFs between the bare beam and the 2 types of metamaterial beams. The vertical lines represent the predicted stop band limits, shown in Table 4 and are coloured according to the colour of their respective FRF.
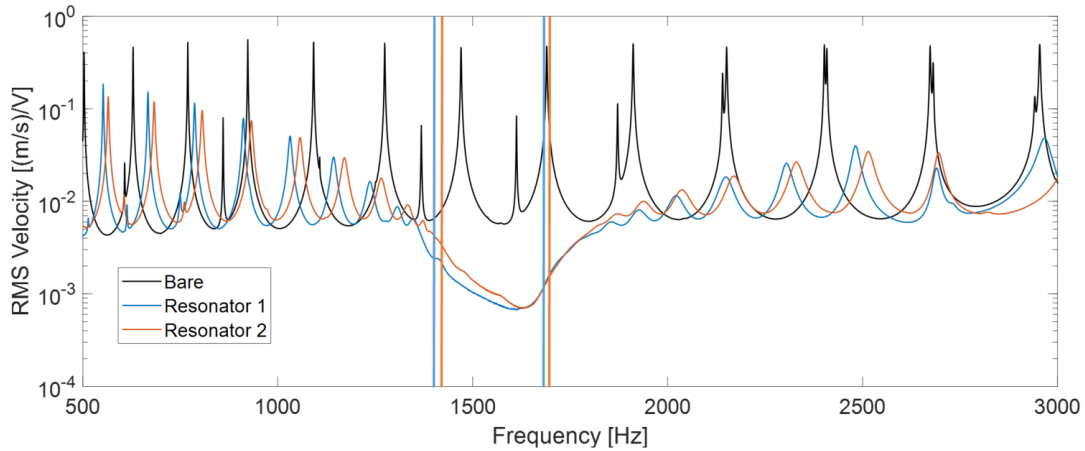
Figure 15: Comparison of experimental FRFs for the bare beam and the beams with resonators. The vertical lines represent the predicted stop band limits.

An improvement in the vibration response can be seen in the predicted stop band regions for the 2 types of resonators. In addition, for the metamaterial beam type 1, the region of improvement is wider and outperforms metamaterial beam type 2, even though resonators type 2 are heavier than type 1 which, for a same tuned frequency, could lead to a wider stop band [9].

4. CONCLUSION

In this paper, the footprint of a resonator was shown to be a parameter that does not only affect the width of a stop band but also the stop band location in the frequency domain. On the one hand, stop bands tend to be wider as the footprint of the resonant additions on the host structure decreases. On the other hand, these zones tend to shift to higher frequencies as the value of the footprint increases. This was shown both through a numerical example of academic spring mass systems as by an experimental validation on 1D beams.

5. ACKNOWLEDGEMENTS

6. REFERENCES

1. Claeys, C., et al. *Design and validation of metamaterials for multiple structural stop bands in waveguides.* Extreme Mechanics Letters 12, 7-22 (2017).
2. Nateghi, A., et al. *Wave propagation in locally resonant cylindrically curved metamaterial panels.* International Journal of Mechanical Sciences 127, 73-90 (2017).
3. de Melo Filho, N. G. R., et al. *Dynamic mass based sound transmission loss prediction of vibro-acoustic metamaterial double panels applied to the mass-air-mass resonance.* Journal of Sound and Vibration (2018).

4. Nouh, M., et al. *Wave propagation in metamaterial plates with periodic local resonances.* Journal of Sound and Vibration 341 (2015): 53-73.

5. Claeys, C. *Design and analysis of resonant metamaterials for acoustic insulation* (Ontwerp en analyse van resonante metamaterialen voor geluidsisolatie), KU Leuven, PhD thesis (2014).

6. Liu, Z., et al. *Locally resonant sonic materials.* Science 289.5485 (2000).

7. Wang, Gang, et al. *Two-dimensional locally resonant phononic crystals with binary structures.* Physical review letters 93.15 (2004).

8. Goffaux, C., et al. *Evidence of Fano-like interference phenomena in locally resonant materials.* Physical review letters 88.22 (2002).

9. Claeys, C., et al. *On the potential of tuned resonators to obtain low-frequency vibrational stop bands in periodic panels.* Journal of Sound and Vibration 332.6 1418-1436 (2013).

10. Brillouin, L. *Wave propagation in periodic structures: electric filters and crystal lattices.* Courier Corporation (2003).

11. Hussein, I. *Reduced Bloch mode expansion for periodic media band structure calculations.* Proceedings of the Royal Society of London A: Mathematical, Physical and Engineering Sciences. The Royal Society, 2009.

12. Van Belle, L., et al. *On the impact of damping on the dispersion curves of a locally resonant metamaterial: Modelling and experimental validation.* Journal of Sound and Vibration 409, 1-23 (2017).

13. Krushynska, A. O. et al. *Towards optimal design of locally resonant acoustic metamaterials.* Journal of the Mechanics and Physics of Solids 71, 179-196 (2014).

14. Sangiuliano, L., et al. *On the influence of boundary conditions on the predicted stop band width of finite size locally resonant metamaterials.* 13th International Conference on Theoretical and Computational Acoustics, ICTCA 2017; 2017; Vol. 2017-July; pp. 99.

15. Liu, X. N., et al. *Wave propagation characterization and design of two-dimensional elastic chiral metacomposite.* Journal of Sound and Vibration 330.11, 2536-2553 (2011).

16. Wijker, J. J. *Spacecraft structures*. Springer Science & Business Media (2008).

17. Mace, B. R., Manconi E. *Modelling wave propagation in two-dimensional structures using finite element analysis.* Journal of Sound and Vibration, Vol. 318, No. 4-5, 884–902 (2008).

18. Mead, D. *Wave propagation in continuous periodic structures: research contributions from southampton*,1964–1995, Journal of sound and vibration, Vol. 190, No. 3, 495–524 (1996).

19. Mace, B. R., et al, *Finite element prediction of wave motion in structural waveguides*, The Journal of the Acoustical Society of America, Vol. 117, No. 5, 2835–2843 (2005).

20. Chen, J. S., et al. *Flexural wave propagation in metamaterial beams containing membrane-mass structures.* International Journal of Mechanical Sciences 131, 500-506 (2017).

21. Sangiuliano, L., et al. *Control of edge modes in finite vibro-acoustic resonant metamaterials.* ISMA-USD Noise and Vibration Engineering Conference (2018).